NREL
Transforming ENERGY

Automated Post-Mold Operations for Wind Blade Manufacturing

Hunter Huth

NAWEA/WindTech 2023
10/30/2023

Contents

What Is The Finishing Process?

- Blades are made in two composite blade halves

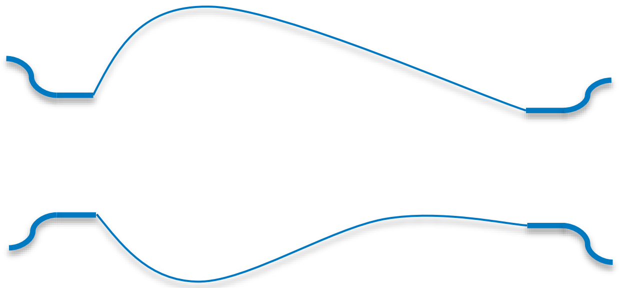

What Is The Finishing Process?

- Blades are made in two composite blade halves
- The blade skins are glued together resulting in flashing at the leading-/trailing-edge

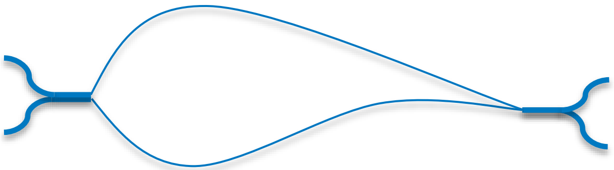

What Is The Finishing Process?

- Blades are made in two composite blade halves
- The blade skins are glued together resulting in flashing at the leading-/trailing-edge
- The flashing is trimmed close to the blade to remove the majority of material

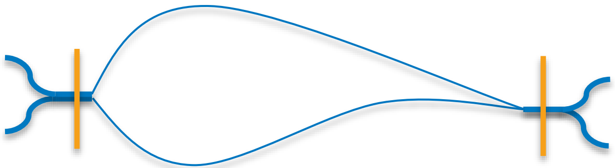

What Is The Finishing Process?

- Blades are made in two composite blade halves
- The blade skins are glued together resulting in flashing at the leading-/trailing-edge
- The flashing is trimmed close to the blade to remove the majority of material
- The leftover “nose” material after trimming is grinded to produce the desired shape

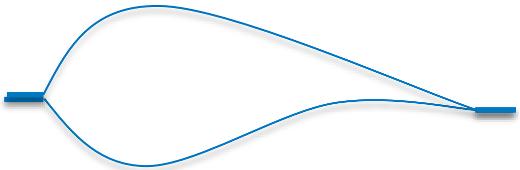

What Is The Finishing Process?

- Blades are made in two composite blade halves
- The blade skins are glued together resulting in flashing at the leading-/trailing-edge
- The flashing is trimmed close to the blade to remove the majority of material
- The leftover "nose" material after trimming is grinded to produce the desired shape
- The leading and trailing edge areas are sanded to prepare for applying protective material

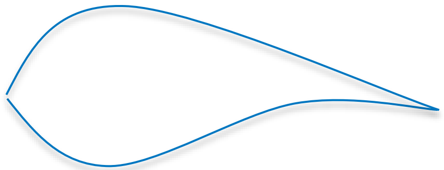

Why automate wind blade finishing?

- The Workforce Institute (2022) found that skilled labor shortages affected 77% of manufacturers' ability to meet production demands
  - Improving worker safety and well-being is a priority for strengthening the workforce

Photo by Casey Nichols

Why automate wind blade finishing?

- The Workforce Institute (2022) found that skilled labor shortages affected 77% of manufacturers' ability to meet production demands
  - Improving worker safety and wellbeing is a priority for strengthening the workforce
- Shields et al. (2023) determined the United States will need 5 additional blade manufacturing facilities to meet offshore wind production goals
  - Automation can change the cost differential between foreign and domestically manufactured blades

Photo by Casey Nichols

Why automate wind blade finishing?

- The Workforce Institute (2022) found that skilled labor shortages affected 77% of manufacturers' ability to meet production demands
  - Improving worker safety and wellbeing is a priority for strengthening the workforce
- Shields et al. (2023) determined the U.S. will need 5 additional blade manufacturing facilities to meet Offshore Wind production goals
  - Automation can change the cost differential between foreign and domestically manufactured blades
- Significantly reduce manufacturing cycle time
  - Laborers can focus on other process such as layup and infusion

Photo by Casey Nichols

Robot Cell Overview

Image taken by Hunter Huth

Robot Hardware Overview

- KUKA KR300R2500 Ultra (2021) with linear track
  - 2.5m Reach, 300 Kg payload, 6.6m track

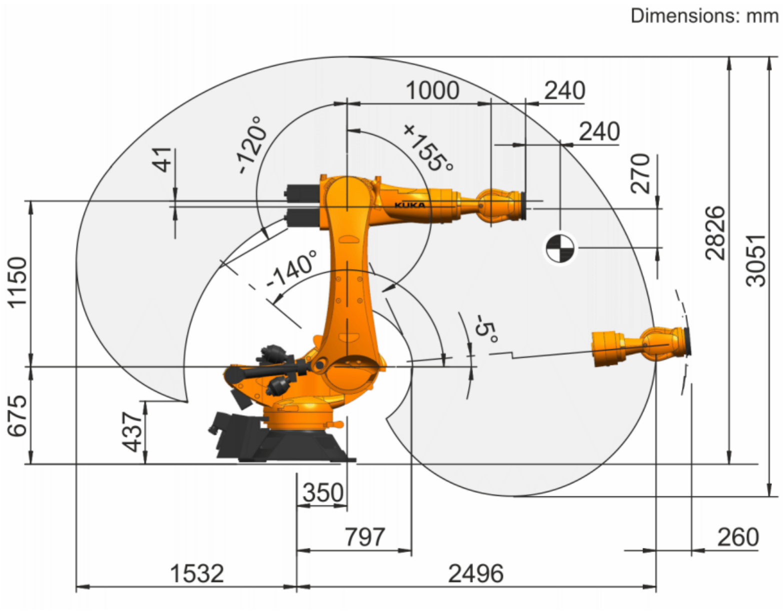

Photo from KUKA KR300R2500

Robot Hardware Overview

- KA KR300R2500 ultra (2021) with linear track
  - 2.5m Reach, 300 Kg payload, 6.6m track
- Zivid II (2023) Structured Light Camera
  - 55 µm point precision

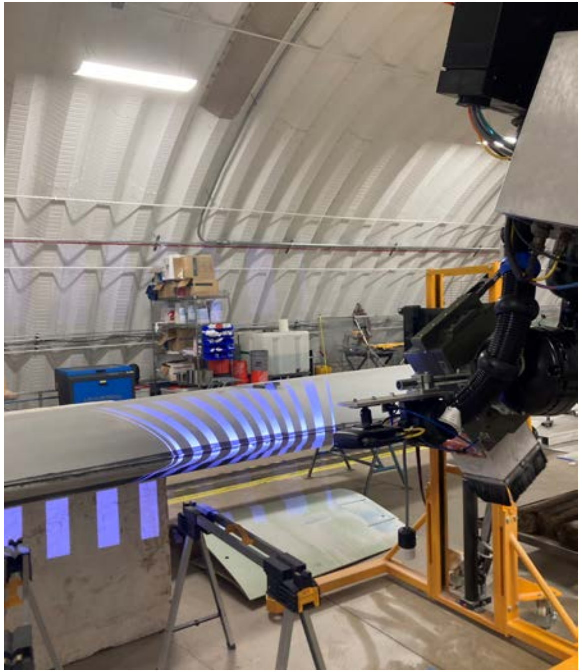

Photo by Hunter Huth

Robot Hardware Overview

- Kuka KR300R2500 with linear track
  - 2.5m Reach, 300 Kg payload, 6.6m track
- Zivid II Structured Light Camera
  - 55 µm point Precision
- Pushcorp (2020) AFD 1240 active compliance device with STC1515 spindle
  - 36 mm carriage travel, .8 lb force resolution

Photo from Pushcorp (https://pushcorp.com/product/afd1240/)

Software was built using the open-source Robot Operating System (ROS 2009)

- Modular framework that separates functions into nodes

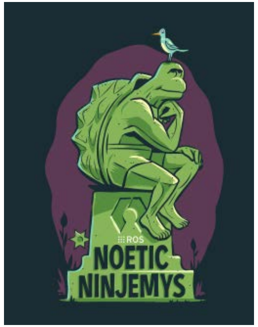

Photo from wiki.ros.org

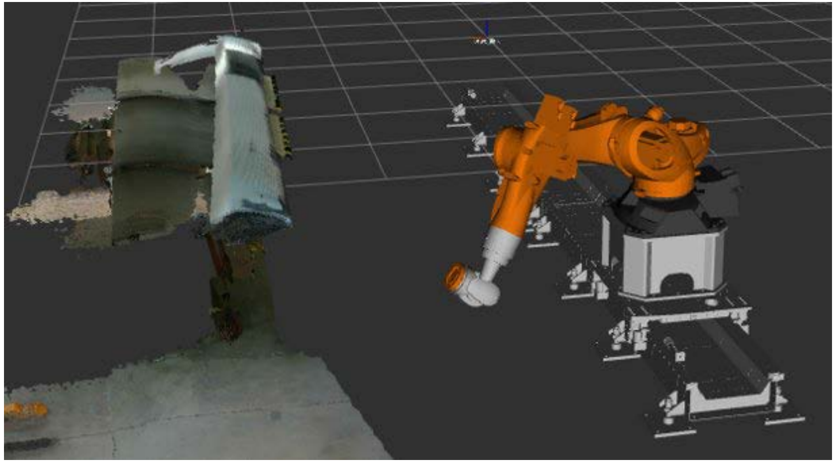

Screen capture of Rviz by Hunter Huth

Software was built using the open-source Robot Operating System (ROS, 2009)

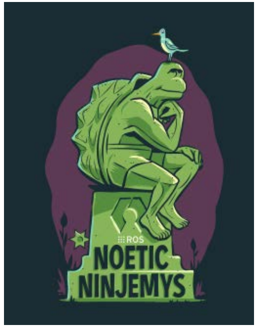

Photo from wiki.ros.org

- Modular framework that separates functions into nodes
- Handles communication between nodes with publish/subscription to topics

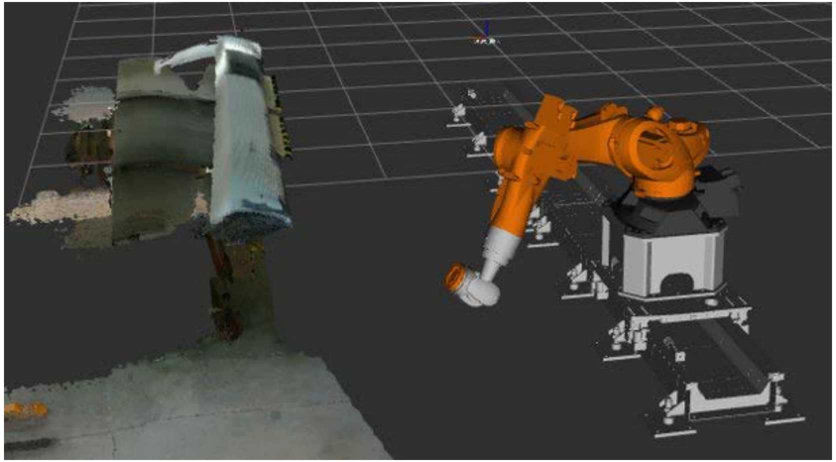

Screen capture of Rviz by Hunter Huth

Software was built using the open-source Robot Operating System (ROS, 2009)

- Modular framework that separates functions into nodes
- Handles communication between nodes with publish/subscription to topics
- Includes tools for development, debugging, and visualization
  - RViz (2015) allows real time visualizing of robot processes

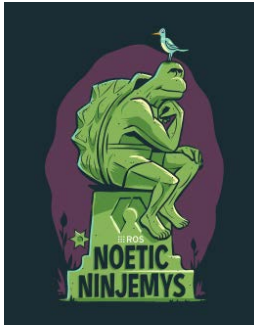

Photo from wiki.ros.org

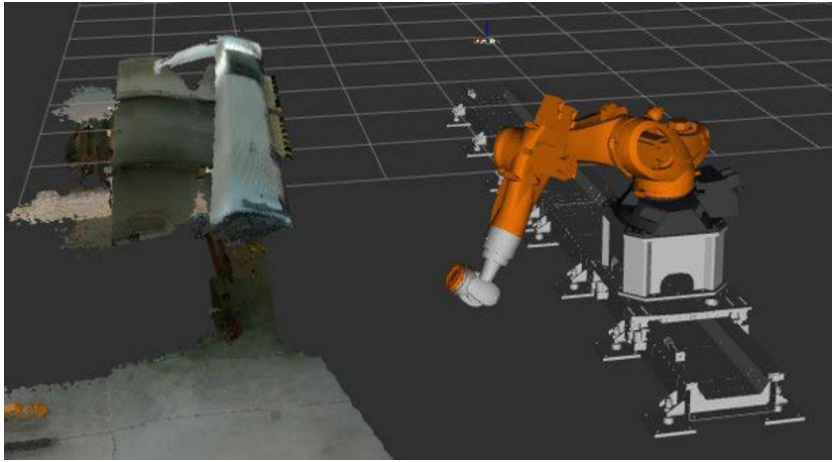

Screen capture of Rviz by Hunter Huth

Process Overview

Global Scan	• Identifies position of blade
Local Scan	• Captures up-close data for toolpath generation
Leading/Trailing Edge Detection	• Identifies important features for toolpath generation
Toolpath Generation	• Toolpath generators for trimming, grinding, and sanding
Toolpath Execution	• Executes spline trajectory received from toolpath generator

Capturing blade geometry is a two-step process

- A global scan captures 3D point cloud data of the entire scene
- Blade position is determined by scene segmentation
- A local scan that scans the leading/trailing edge at the optimal distance for the Zivid II camera

4x – speed

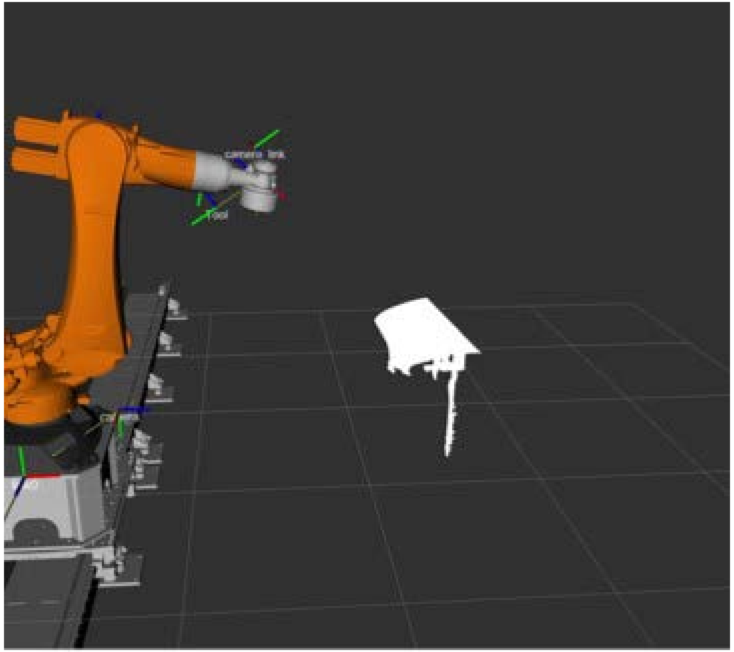

Screen record of Rviz by Hunter Huth

Trimming Operation

Photo taken by Hunter Huth

First step is to identify the boundary between the flashing and the blade

- A moving least squares (MLS) implemented through the point cloud library (PCL 2011) is used to fit a smooth surface to the blade.
- The cloud is sliced in the span-wise direction.
- Normal vectors in the chord-wise direction are calculated and analyzed to find large changes in the normal at the leading edge/flashing boundary

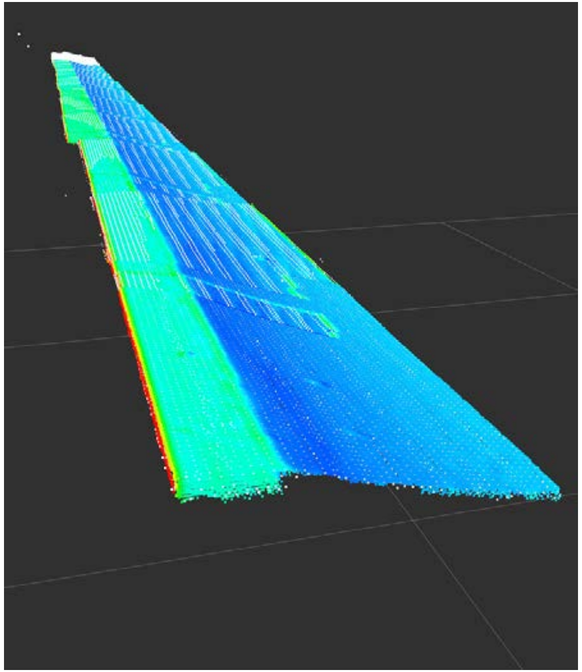

Screen capture of Rviz by Hunter Huth

Normal vectors are analyzed to find the flashing boundary

- Normal components in chord-wise direction are calculated along the chord seen in top plot

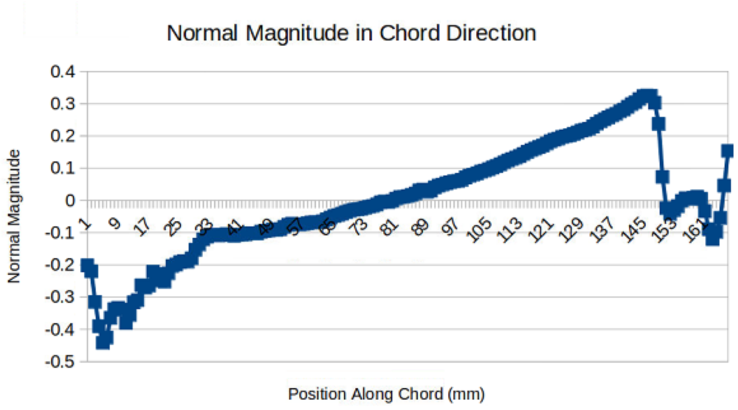

Normal vectors are analyzed to find the flashing boundary

- Normal components in chord-wise direction are calculated along the chord seen in top plot
- Difference between adjacent normal vector magnitudes are calculated along the chord seen in bottom plot
  - Analogous to 1st derivative

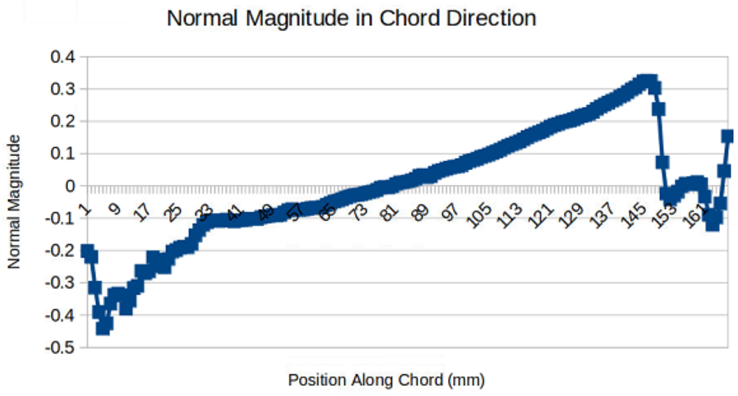

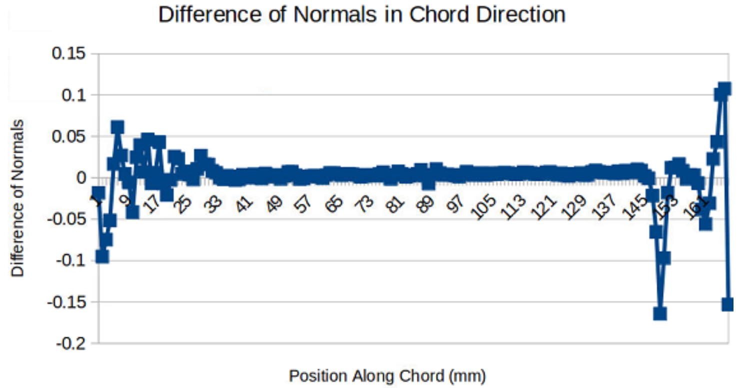

Normal vectors are analyzed to find the flashing boundary

- Normal components in chord-wise direction are calculated along the chord seen in top plot
- Difference between adjacent normal vector magnitudes are calculated along the chord seen in bottom plot
  - Analogous to 1st derivative
- The flashing begins at the horizontal line found through reducing high frequency noise and finding absolute maximum

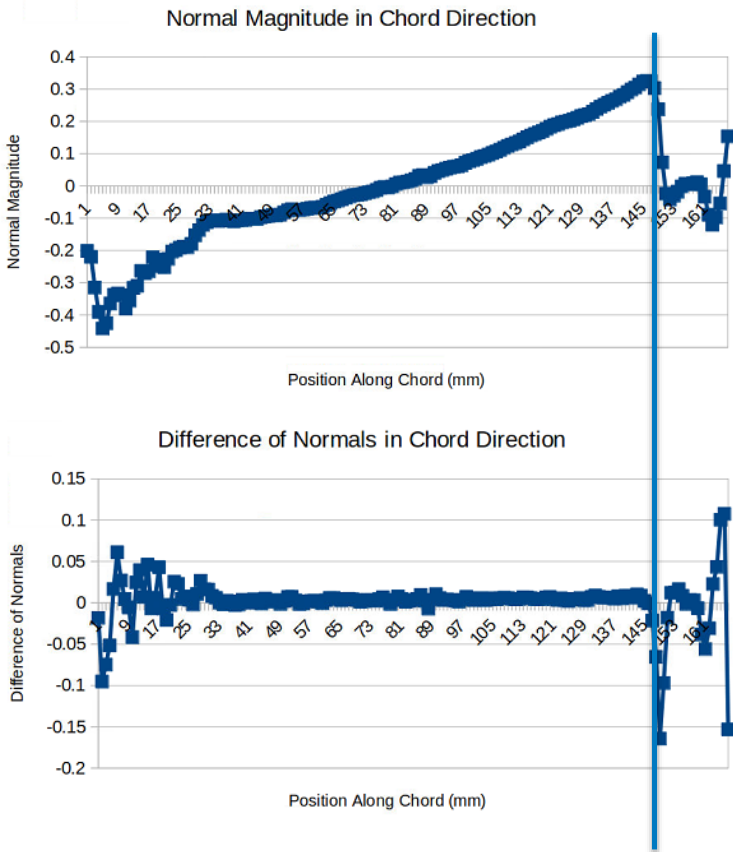

Trimming toolpath calculated from the leading/trailing edge

- An offset is added to prevent damage to the blade

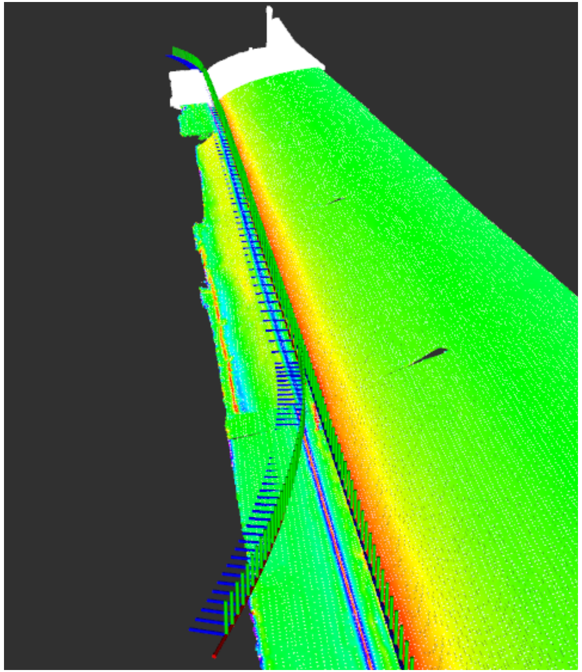

Screen capture of Rviz by Hunter Huth

Trimming toolpath calculated from the leading/trailing edge

- An offset is added to prevent damage to the blade
- Lead-ins and lead-outs are added every 2.5 m to separate hanging flashing

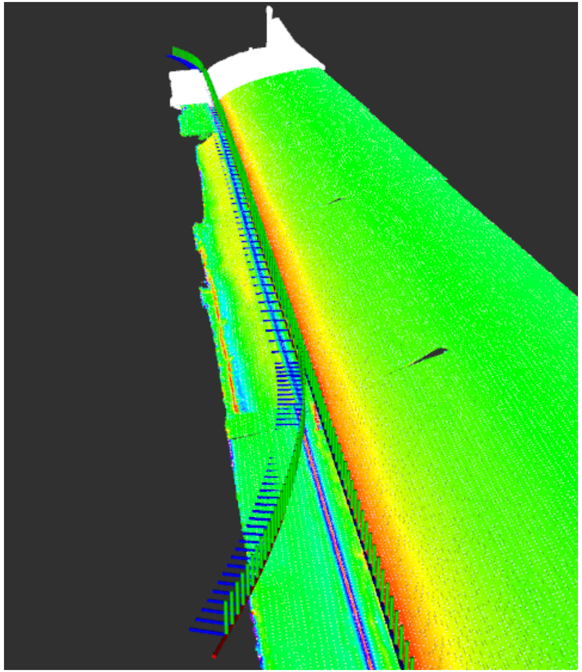

Screen capture of Rviz by Hunter Huth

Trimming toolpath calculated from the leading/trailing edge

- An offset is added to prevent damage to the blade
- Lead-ins and lead-outs are added every 2.5m to separate hanging flashing
- This toolpath is passed as a spline trajectory to the robot controller

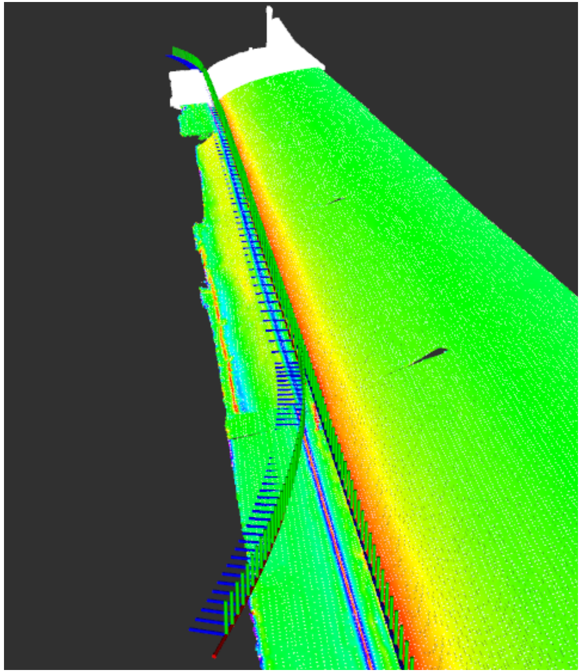

Screen capture of Rviz by Hunter Huth

Trimming Execution

Leading Edge – 4x speed

Trailing Edge - 4x speed

Videos by Hunter Huth

Trimming Results

- Operation speed of .96 m/min and 1.09 m/min for leading and trailing edge respectively

Leading Edge	
Process Step	Time (minutes)
Global Scan	0.48
Global Blade Detection	0.32
Local Scan	0.60
Toolpath Generation	0.59
Toolpath Execution	3.19

Trailing Edge	
Process Step	Time (minutes)
Global Scan	0.61
Global Blade Detection	0.15
Local Scan	0.61
Toolpath Generation	0.38
Toolpath Execution	2.82

- Accuracy of -4.5/+0.7 mm and -3.1/+ 3.6 mm for leading and trailing edge respectively

Photo by Hunter Huth

Grinding Operation

Photo by Hunter Huth

Identifying leftover nose material after trimming from point cloud

- Slice leading edge area into 2D cross sections

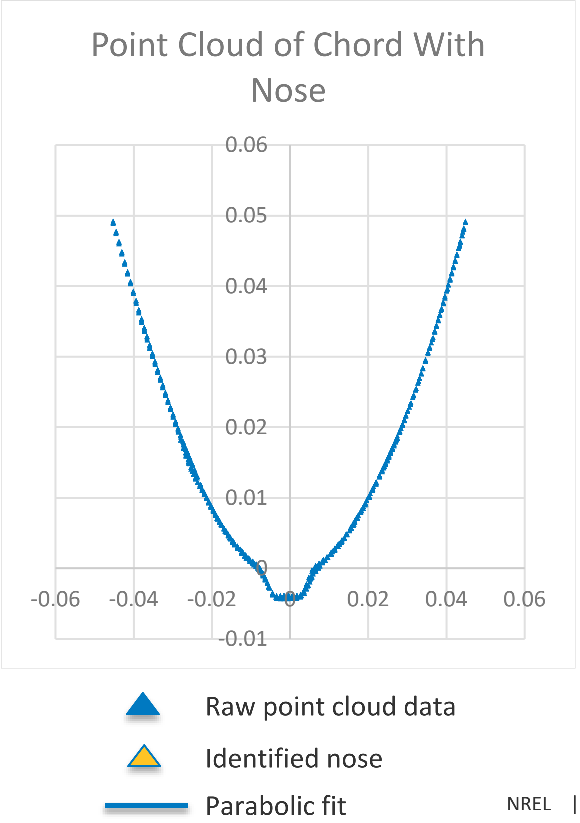

Identifying leftover nose material after trimming from point cloud

- Slice leading edge area into 2D cross sections
- Fit a parabola along the leading-edge chord.

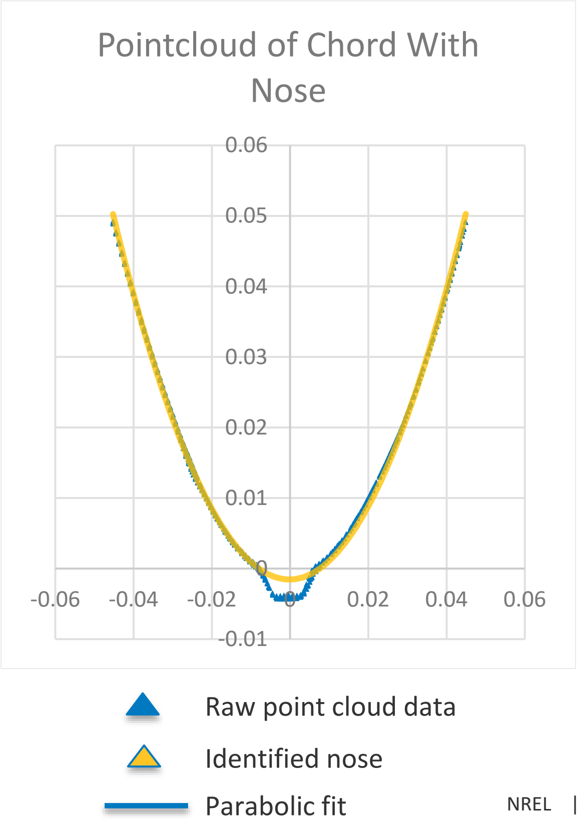

Identifying leftover nose material after trimming from point cloud

- Slice leading edge area into 2D cross sections
- Fit a parabola along the leading-edge chord.
- Use parabola minimum as leading edge

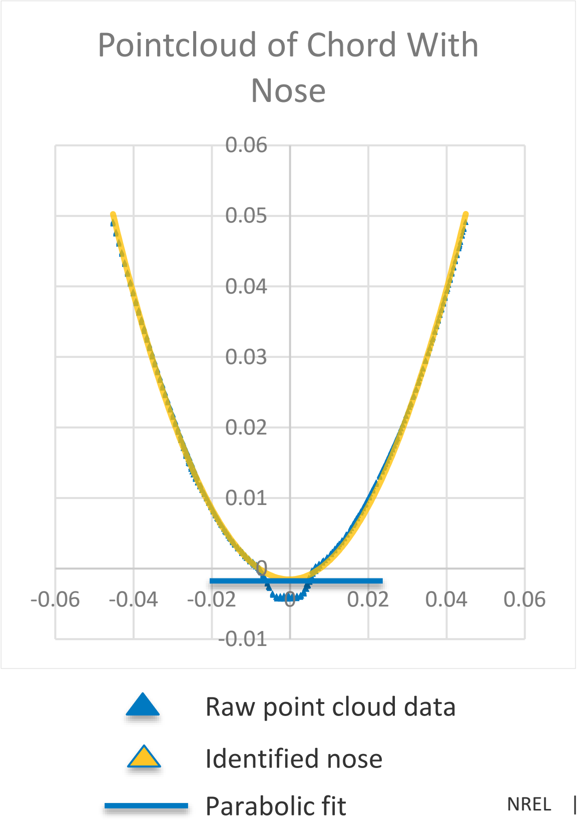

Identifying leftover nose material after trimming from point cloud

- Slice leading edge area into 2D cross sections
- Fit a parabola along the leading-edge chord.
- Use parabola minimum as leading edge
- Extract nose points below parabola minimum

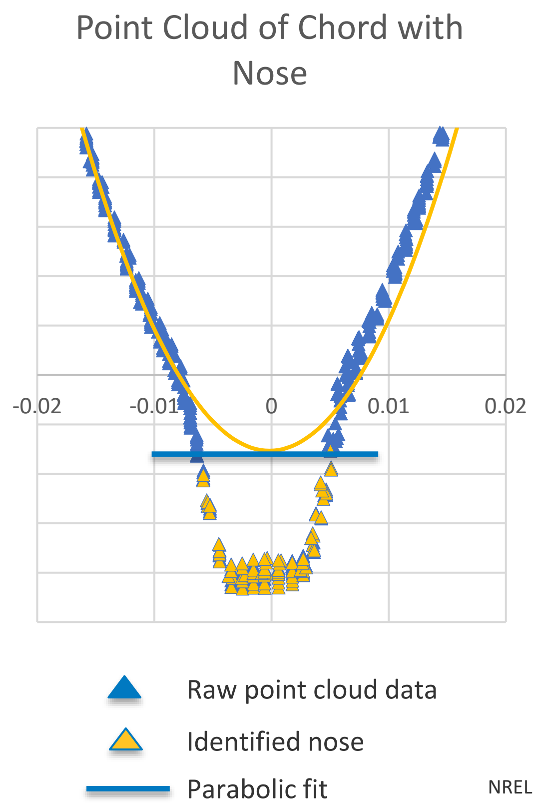

Identifying leftover nose material after trimming from point cloud

- Slice leading edge area into 2D cross sections
- Fit a parabola along the leading-edge chord.
- Use parabola minimum as leading edge
- Extract nose points below parabola minimum
- Nose thickness (N_t) is the average y-distance to the leading edge
- Nose width (N_w) is the range of nose points in the x-direction

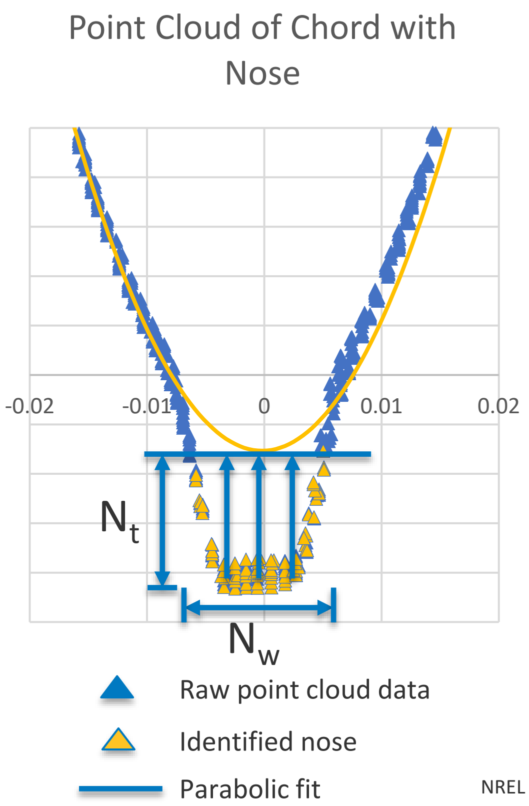

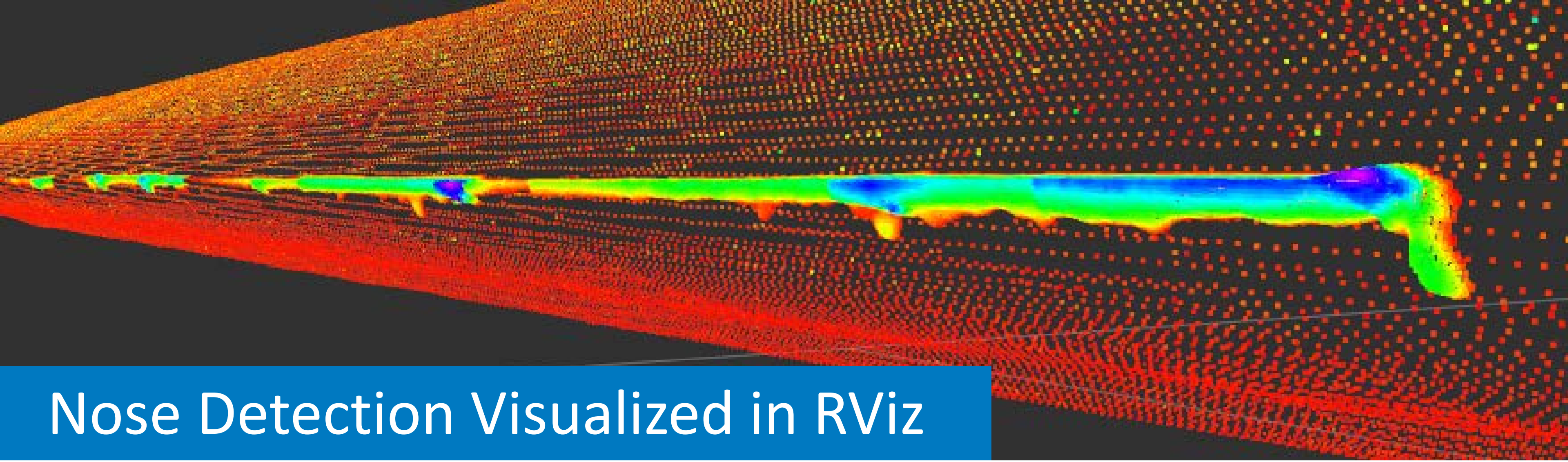

Nose Detection Visualized in RViz

- Outputs
  - Path of the leading edge to follow
  - Size of the nose to be removed
- Need to determine velocity to remove desired amount of material

Screen capture of Rviz by Hunter Huth

Grinding model for calculating travel velocity

- Determines linear travel speed to grind to a certain depth
- On first contact, pressure is high, so grinding depth increases
- Pressure decreases as grinder plunges into material until a steady-state depth is reached

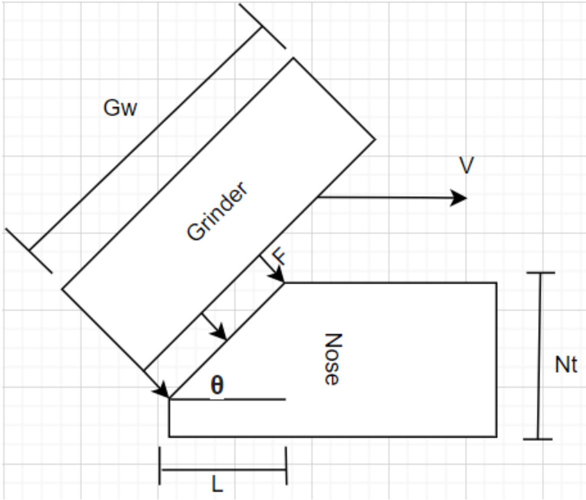

G_w = grinder width
F = force
V = linear velocity
Θ = grinding angle
L = contact length
N_t = nose thickness
N_w = nose width
t = grind time
μ = removal constant

Grinding model for calculating travel velocity

$$L = \frac{N_t}{\tan(\theta)}, \qquad t = \frac{L}{V} = \frac{N_t}{R} = \frac{N_t}{\tan(\theta) * V}$$

Time each slice is in contact with grinder

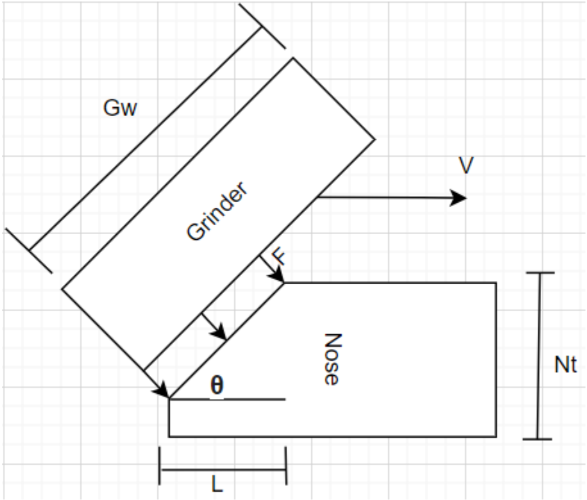

G_w = Grinder Width

F = force

V = linear velocity

Θ = grinding angle constant

L = contact length

N_t = nose thickness

N_w = nose width

t = grind time

μ = removal

Grinding model for calculating travel velocity

$$L = \frac{N_t}{\tan(\theta)}, \qquad t = \frac{L}{V} = \frac{N_t}{R} = \frac{N_t}{\tan(\theta) * V}$$

Time each slice is in contact with grinder

$$V = \frac{R}{\tan(\theta)}, \qquad R = \frac{F}{A} * \mu, \qquad A = Nw * N_t * \sin(\theta)$$

Rate at which material is removed

Contact area of grinder and nose

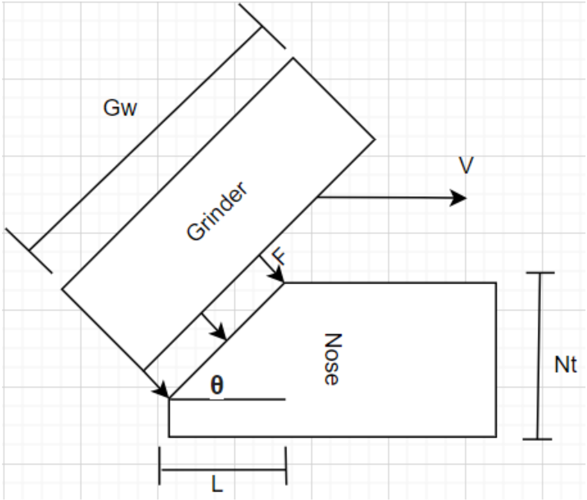

G_w = *Grinder Width*

F = force

V = linear velocity

Θ = grinding angle constant

L = contact length

N_t = *nose thickness*

N_w = *nose width*

t = grind time

μ = removal

Grinding model for calculating travel velocity

$$L = \frac{N_t}{\tan(\theta)}, \qquad t = \frac{L}{V} = \frac{N_t}{R} = \frac{N_t}{\tan(\theta) * V}$$

Time each slice is in contact with grinder

$$V = \frac{R}{\tan(\theta)}, \qquad R = \frac{F}{A} * \mu, \qquad A = Nw*N_t*\sin(\theta)$$

Rate at which material is removed

Contact area of grinder and nose

$$V = \frac{F * \mu * \cos(\theta)}{Nw*Nt}$$

µ characterizes relationship between pressure and removal rate

Linear velocity to remove nose given a grinding angle, force, nose size, and removal constant

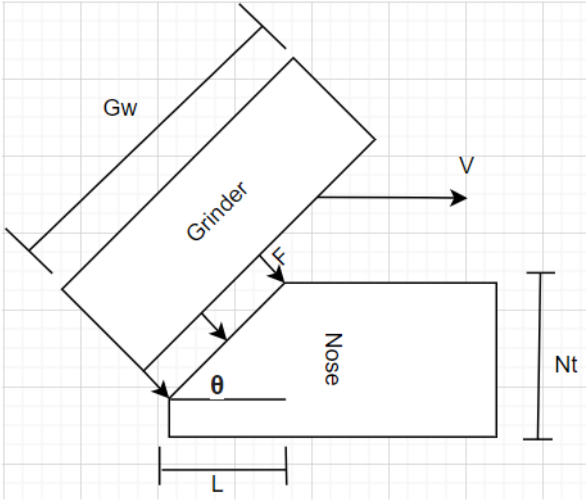

G_w = Grinder Width

F = force

V = linear velocity

Θ = grinding angle constant

L = contact length

N_t = nose thickness

N_w = nose width

t = grind time

μ = removal

Collecting Data For Grinding Model

- Grinder plunged perpendicular into flashing sample panels at varying forces and composite sample thickness
- Measured the speed the grinder plunged into the surface

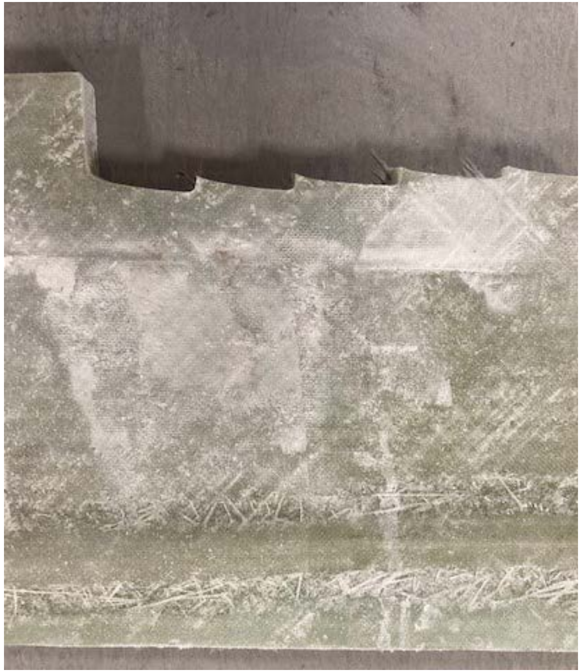

Photo by Hunter Huth

Grinder plunge rates at varying pressure determine removal constant (μ)

- μ = 75.639 $\frac{mm^3}{lb*s}$
- $V = \frac{F*\mu*\cos(\theta)}{Nw*Nt}$
- $V = \frac{F*75.639*\cos(\theta)}{Nw*Nt}$

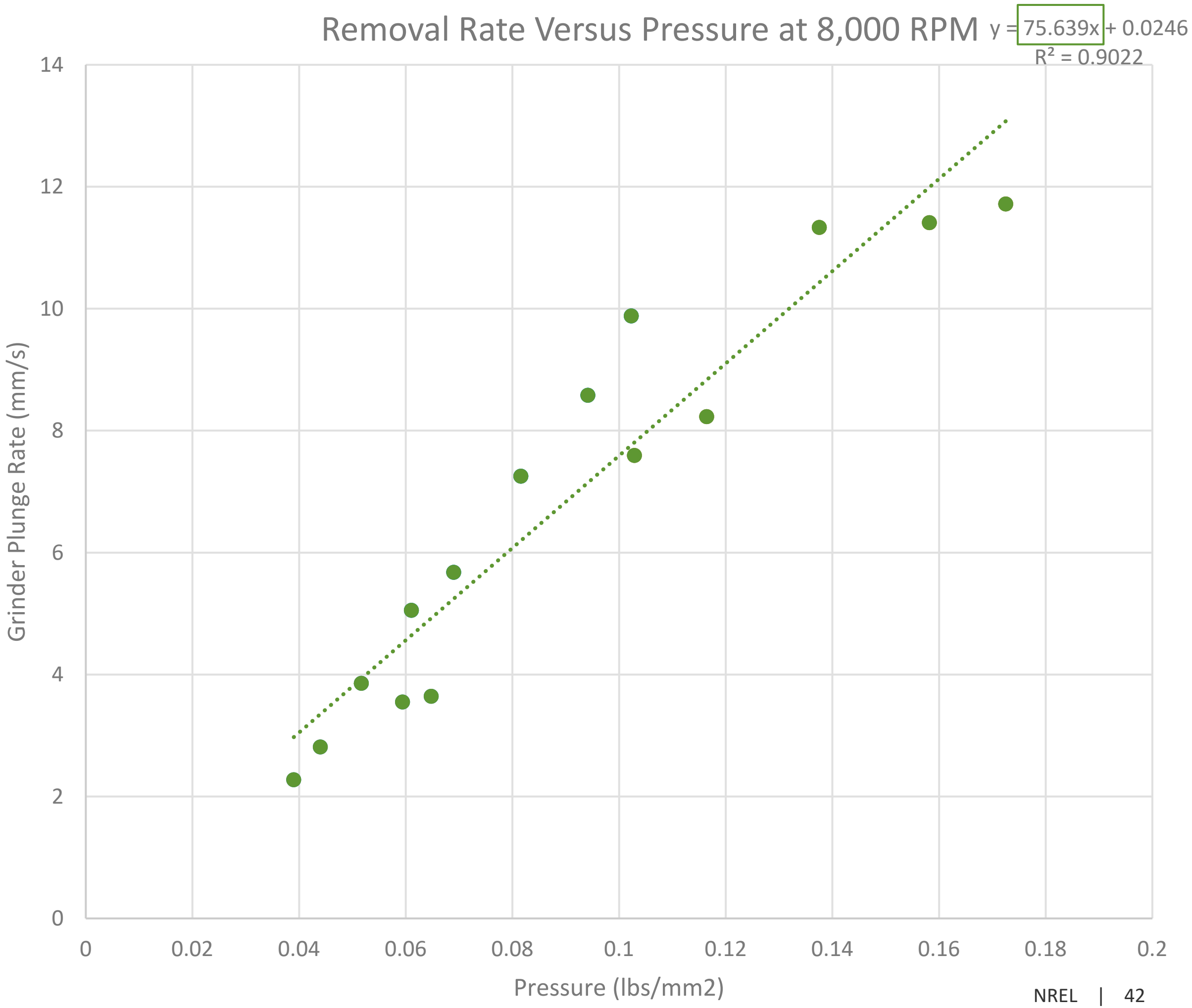

Validated model by performing five 2 mm grinding passes

- Force: 10 lb
- Grind angle: 5°
- Travel Speed 67.28 mm/s
- RPM: 8,000

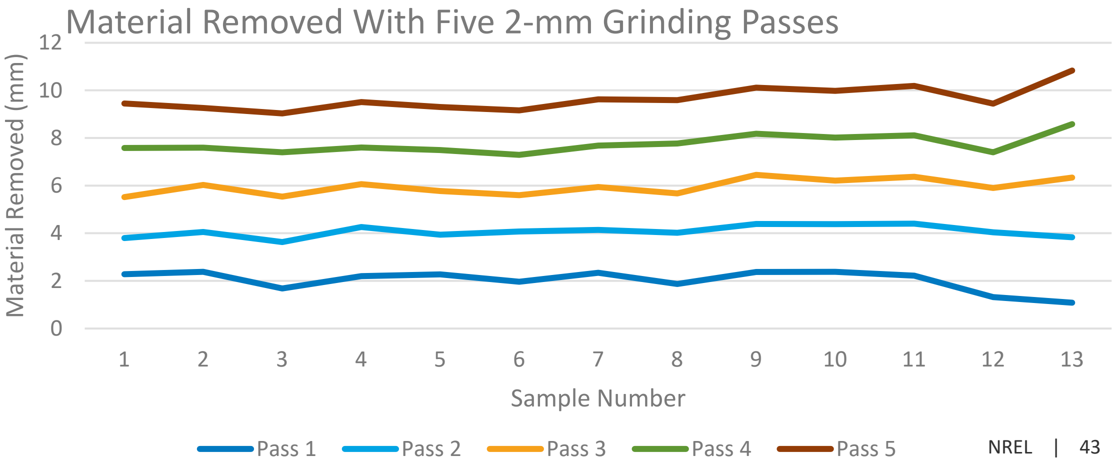

Photo by Hunter Huth

Grinding toolpath executed in multiple passes

- Maximum material removed per pass is 2 mm
- The pass length is optimized for longer passes to get a smooth finish

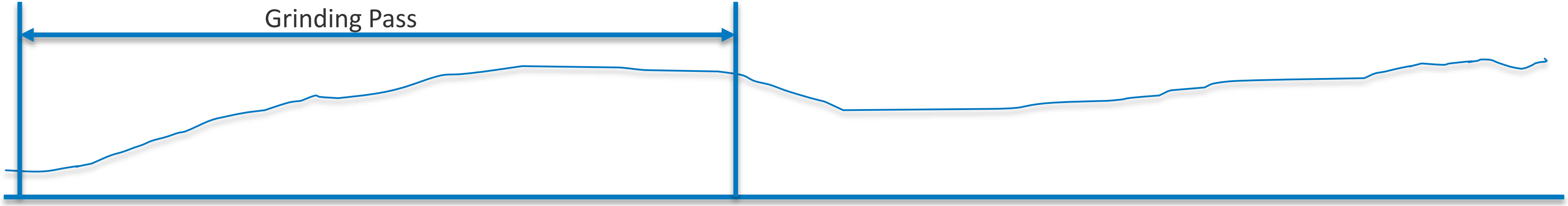

N_t	2	4	6	7	8	7	5	5	7	8	9
Pass 1	0	2	4	5	6	6	5	5	7	8	9
Pass 2											
Pass 3											

Small N_t has only 1 mm removed

End Grinding pass because N_t is smaller than previous max N_t

Grinding toolpath executed in multiple passes

- Maximum material removed per pass is 2mm
- The pass length is optimized for longer passes to get a smooth finish

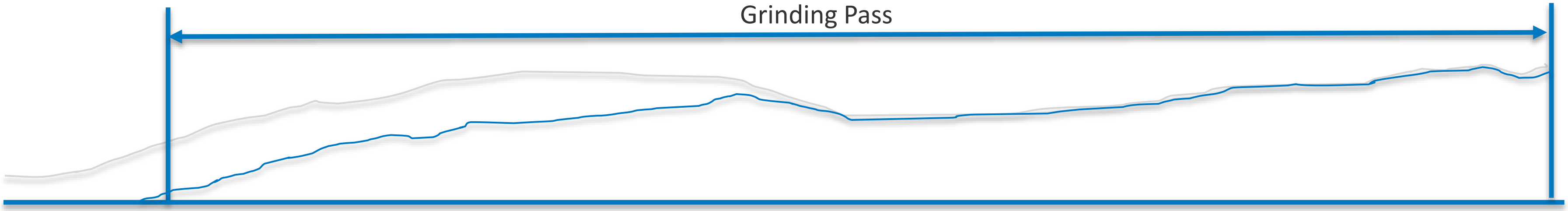

N_t	2	4	6	7	8	7	5	5	7	8	9
Pass 1	0	2	4	5	6	6	5	5	7	8	9
Pass 2	0	0	2	3	4	4	4	4	5	6	7
Pass 3											

Small N_t has only 1 mm removed

Grinding toolpath executed in multiple passes

- Maximum material removed per pass is 2mm
- The pass length is optimized for longer passes to get a smooth finish

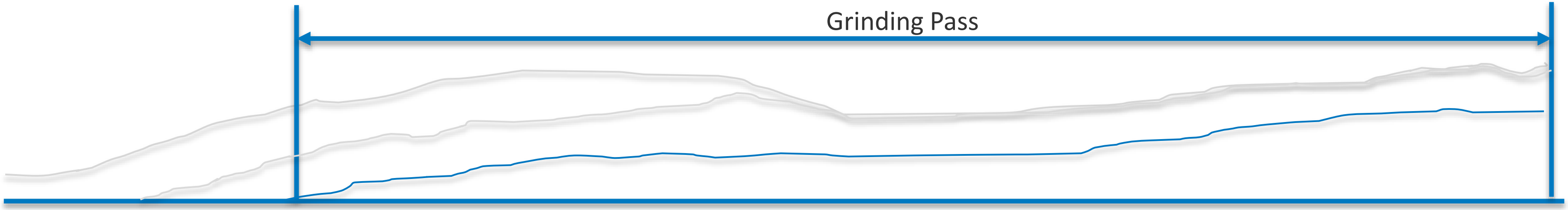

N_t	2	4	6	7	8	7	5	5	7	8	9
Pass 1	0	2	4	5	6	6	5	5	7	8	9
Pass 2	0	0	2	3	4	4	4	4	5	6	7
Pass 3	0	0	0	1	2	2	2	2	3	4	5

Grinding Execution

- Overall process speed of .63 m/min

Process Step	Time (minutes)
Global Scan	0.5
Global Blade Detection	0.2
Local Scan	0.96
Toolpath Generation	0.64
Toolpath Execution	5.61

- Leading edge shape did not meet manufacturing tolerances

2x – speed

Video by Hunter Huth

Grinding Results

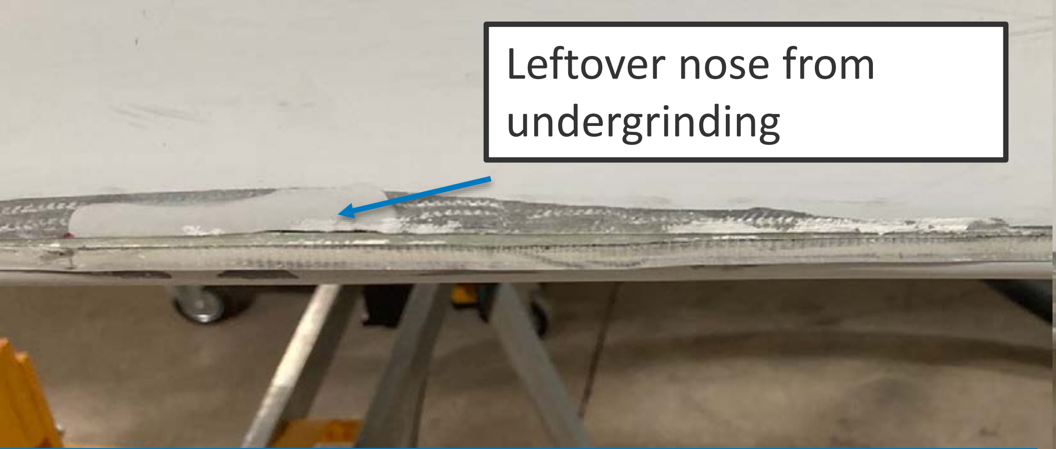

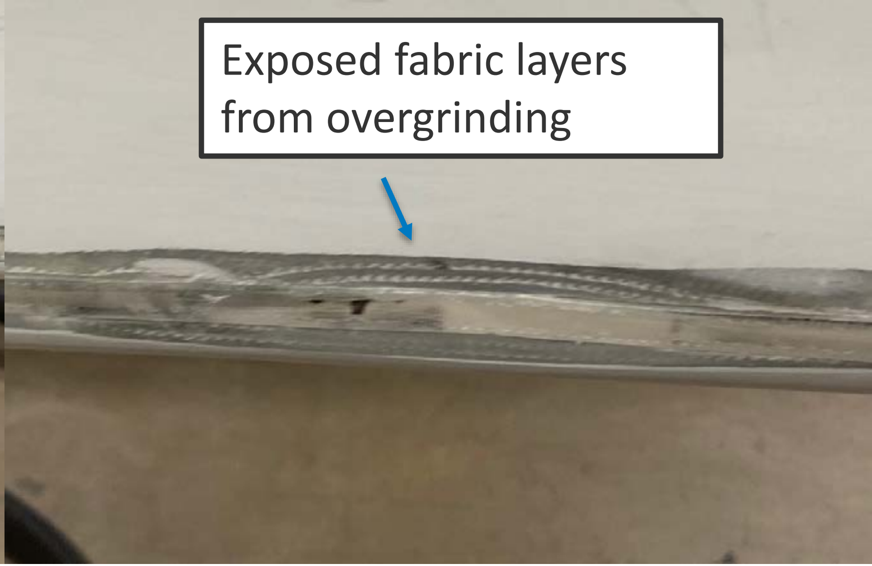

- Results showed areas of over-grinding and under-grinding due to variables unaccounted for in the grinding model
  - Glue thickness versus composite thickness
  - Abrasive degradation
- Future research focus is collecting nose size data after each grinding pass to update grinding model parameters

Photo by Hunter Huth

Sanding Operation

Photo taken by Hunter Huth

Leading- and trailing-edge detection for Sanding Toolpath

- Leading edge is detected through same algorithm as the grinding process

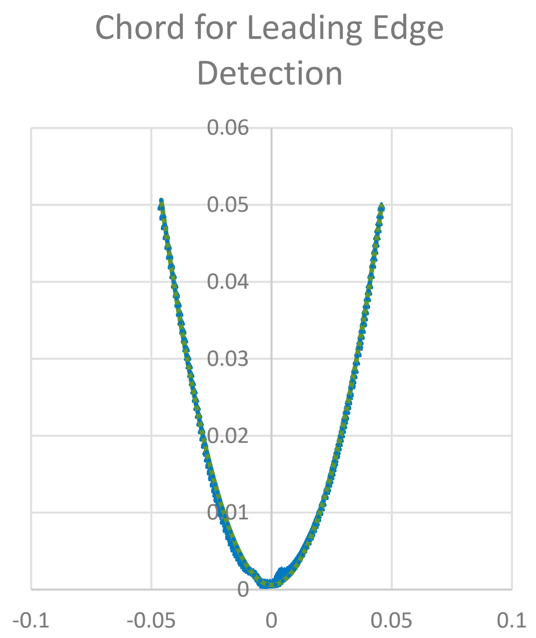

Leading and trailing edge detection for sanding toolpath

- Leading edge is detected through same algorithm as the grinding process
- Trailing edge for sanding is detected with same algorithm as trailing edge trimming
  - Needs scans above and below trailing edge
  - Large change in normal at trailing edge

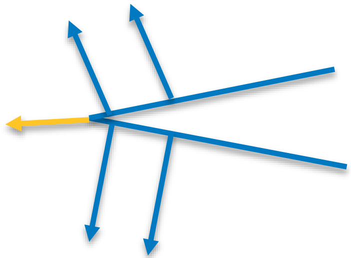

Leading-Edge Sanding Toolpath Generation

- Separate leading-edge chords into sections that match width of sanding drum

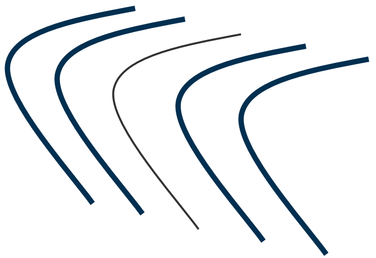

Drawing created by Hunter Huth

Leading-Edge Sanding Toolpath Generation

- Separate leading-edge chords into sections that match width of sanding drum
- Toolpath position follows the middle of the chord

Drawing created by Hunter Huth

Leading-Edge Sanding Toolpath Generation

- Separate leading-edge chords into sections that match width of sanding drum
- Toolpath position follows the middle of the chord
- Toolpath orientation is the average orientation along the chords

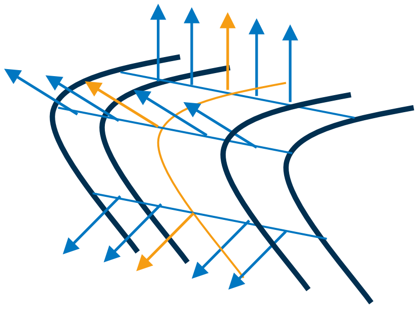

Drawing created by Hunter Huth

Leading Edge Sanding Toolpath Generation

- Separate leading-edge chords into sections that match width of sanding drum
- Toolpath position follows the middle of the chord
- Toolpath orientation is the average orientation along the chords
- Add lead-in/lead-outs for a soft touch with the sander

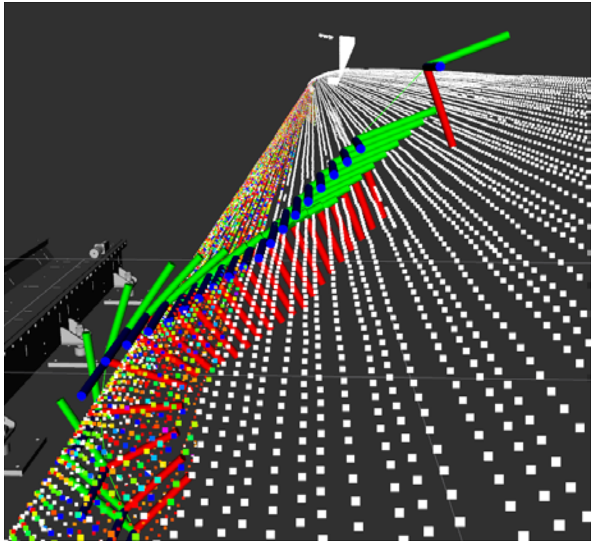

Screen capture of Rviz by Hunter Huth

Trailing Edge Sanding Toolpath Generation

- Trailing-Edge Sanding Toolpath follows the span-wise direction
- The sander angle compared to the trailing edge is calculated to sand the desired chord depth and optimize abrasive usage

Photo by Hunter Huth

Trailing Edge Sanding Toolpath Generation

- Trailing Edge Sanding Toolpath follows the span-wise direction
- The sander angle compared to trailing edge is calculated to sand the desired chord depth and optimize abrasive usage
- The sander orientation is determined by the average normal orientation under the sanding drum

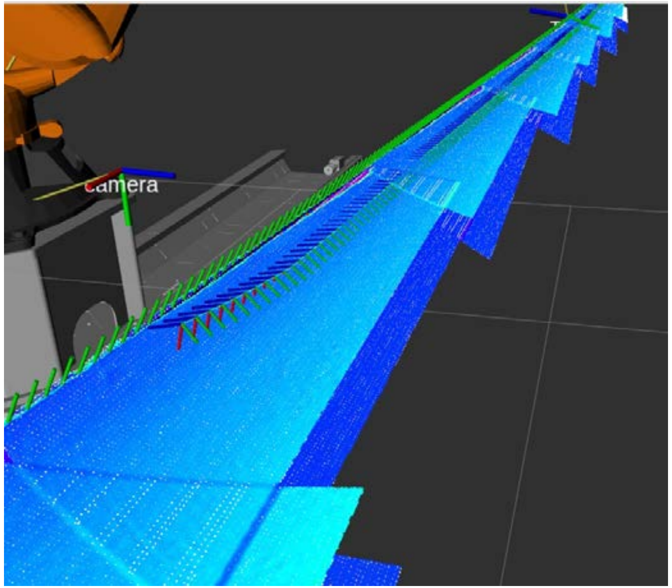

Screen capture of Rviz by Hunter Huth

Sanding Execution

Leading Edge – 4x speed

Trailing Edge – 4x speed

Videos by Hunter Huth

Sanding Results

- The overall speed was .79 m/min for leading edge and .81 m/min for trailing edge respectively

Leading Edge	
Process Step	Time (minutes)
Global Scan	0.68
Global Blade Detection	0.83
Local Scan	0.59
Toolpath Generation	0.2
Toolpath Execution	4.1

Trailing Edge	
Process Step	Time (minutes)
Global Scan	0.85
Global Blade Detection	0.88
Local Scan	1.05
Toolpath Generation	1.30
Toolpath Execution	2.05

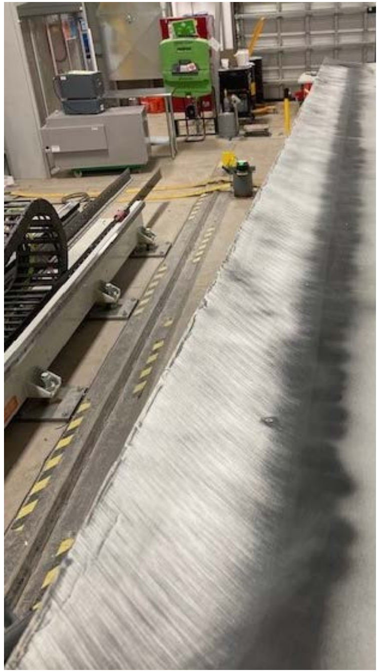

Photos by Hunter Huth

Leading Edge *Trailing Edge*

Sanding Results

- The overall speed was .79 m/min for leading edge and .81 m/min for trailing edge respectively

Leading Edge		Trailing Edge	
Process Step	Time (minutes)	Process Step	Time (minutes)
Global Scan	0.68	Global Scan	0.85
Global Blade Detection	0.83	Global Blade Detection	0.88
Local Scan	0.59	Local Scan	1.05
Toolpath Generation	0.2	Toolpath Generation	1.30
Toolpath Execution	4.1	Toolpath Execution	2.05

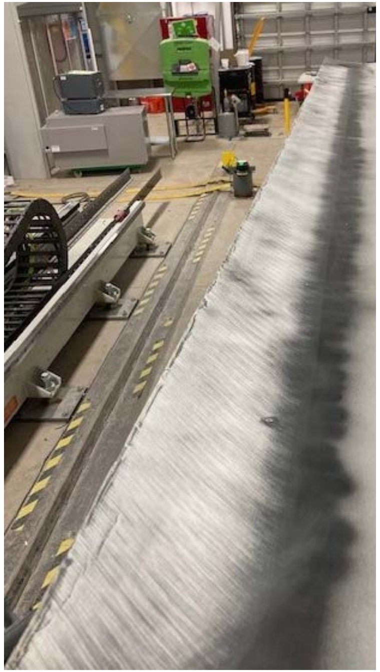

Photos by Hunter Huth

Leading Edge

Trailing Edge

Sanding Results

- The overall speed was .79 m/min for leading edge and .81 m/min for trailing edge respectively

Leading Edge		Trailing Edge	
Process Step	Time (minutes)	Process Step	Time (minutes)
Global Scan	0.68	Global Scan	0.85
Global Blade Detection	0.83	Global Blade Detection	0.88
Local Scan	0.59	Local Scan	1.05
Toolpath Generation	0.2	Toolpath Generation	1.30
Toolpath Execution	4.1	Toolpath Execution	2.05

- Both operations achieved full coverage of the surface

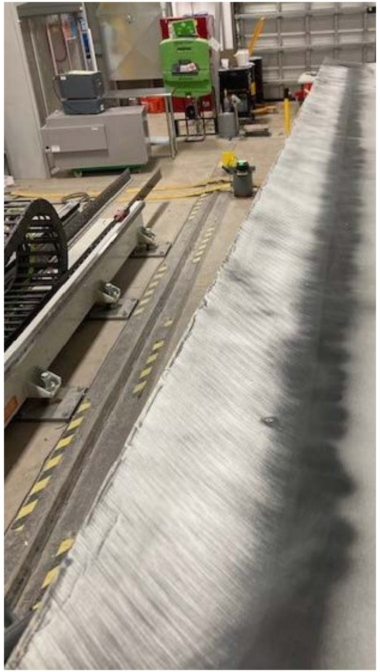

Photos by Hunter Huth

Leading Edge *Trailing Edge*

Future Work

- Increase operational speed through real-time trajectory planning
  - Operation time limited only by max operation speed of tool

Future Work

- Increase operational speed through real time trajectory planning
  - Operation time limited by only max operation speed of tool
- Real-time quality feedback to ensure high performance
  - Inspect operation quality immediately to improve results, such as the leading-edge shape for grinding
  - Tool condition monitoring

Future Work

- Increase operational speed through real time trajectory planning
  - Operation time limited by only max operation speed of tool
- Real time quality feedback to ensure high performance
  - Inspect operation quality immediately to improve results, such as the leading-edge shape for grinding
  - Tool condition monitoring
- Focus testing on the root and tip areas of wind blades

Conclusions

- Implemented automated wind blade finishing processes for trimming grinding, and sanding

	Operational Speed (m/min)	
	Leading Edge	Trailing Edge
Trim	0.96	1.09
Grind	0.63	N/A
Sand	0.79	0.81

Conclusions

- Implemented automated wind blade finishing processes for trimming grinding, and sanding
- Successful results in trimming and sanding
  - Grinding requires real-time feedback for remaining material after each pass

	Operational Speed (m/min)	
	Leading Edge	Trailing Edge
Trim	0.96	1.09
Grind	0.63	N/A
Sand	0.79	0.81

Conclusions

- Implemented automated wind blade finishing processes for trimming grinding, and sanding
- Successful results in trimming and sanding
  - Grinding requires real time feedback for remaining material after each pass
- Future work will focus on speeding up operations and improving finish quality

	Operational Speed (m/min)	
	Leading Edge	Trailing Edge
Trim	0.96	1.09
Grind	0.63	N/A
Sand	0.79	0.81

Acknowledgements

- Automated wind blade finishing team at NREL
  - David Snowberg, Casey Nichols, Derek Berry, Scott Lambert, Petr Sindler, Ryan Beach, and David Barnes
- Department of Energy’s Advanced Materials & Manufacturing Technology Office
- Radhika Kadam and Ivan Mosegaard from LM Wind Power at GE Vernova, for guidance throughout the design process
- NREL technical support staff for their work throughout the project

Q&A

For Additional Questions: hunter.huth@nrel.gov

www.nrel.gov

NREL/PR-5000-87782

This work was authored by the National Renewable Energy Laboratory, operated by Alliance for Sustainable Energy, LLC, for the U.S. Department of Energy (DOE) under Contract No. DE-AC36-08GO28308. Funding provided by the Department of Energy's Advanced Materials & Manufacturing Technology Office. The views expressed in the article do not necessarily represent the views of the DOE or the U.S. Government.

Photo from iStock-627281636

NREL
Transforming ENERGY

References

Workforce Institute. 2022. "Is Stability In Sight?" Accessed 10/14/2023. https://workforceinstitute.org/wp-content/uploads/2022-Manufacturing-Survey_final_rev3.pdf

Shields, Matt, Stefek, Jeremy, Oteri, Frank, Kreider, Matilda, Gill, Elizabeth, Maniak, Sabina, Gould, Ross, Malvik, Courtney, Tirone, Sam, and Hines, Erik. 2023. *A Supply Chain Road Map for Offshore Wind Energy in the United States*. Golden, CO: National Renewable Energy Laboratory. NREL/TP-5000-84710. https://www.osti.gov/servlets/purl/1922189/.

KUKA. 2022. "KUKA KR300R2500 ultra" Accessed 10/14/2023. https://www.kuka.com/-/media/kuka-downloads/imported/8350ff3ca11642998dbdc81dcc2ed44c/0000182713_en.pdf

ZIVID. 2023. "See more. Do more. Zivid Two industrial 3D camera – Zivid" Accessed 10/14/2023. https://www.zivid.com/zivid-2

Pushcorp. 2020. "Leader in Force Compliance, Spindles, and Automation Equipment" Accessed 10/14/2023. https://pushcorp.com/

Quigley, Morgan, Gerkey, Brian, Conley, Ken, Faust, Josh, Foote, Tully, Leibs, Jeremy, Berger, Eric, Wheeler, Rob, and Ng, Andrew. 2009. "ROS: an open-source Robot Operating System." Presented at ICRA Workshop on Open Source Software, http://robotics.stanford.edu/~ang/papers/icraoss09-ROS.pdf

Kam, Hyeong Ryeol, Lee, Sung-Ho, Park, Taejung, Kum, Chang-Hun, 2015, "RViz, a toolkit for real domain data visualization," Telecommunications Systems Volume 60: Pages 337-345, https://doi.org/10.1007/s11235-015-0034-5

Rusu, Radu Bogdan, Cousins, Steve, 2011, "3D is here: Point Cloud Library (PCL)," IEEE International Conference on Robotics and Automation (ICRA), doi: 10.1109/ICRA.2011.5980567